CrossMark

Enthalpy of the $N^+ + H_2 \rightarrow NH^+ + H$ Reaction—Experimental Study of the Reverse Process

Štěpán Roučka[1] ⓘ, Serhiy Rednyk[1] ⓘ, Thuy Dung Tran[1] ⓘ, Artem Kovalenko[1] ⓘ, Dmytro Mulin[1], Sunil S. Kumar[2] ⓘ, Petr Dohnal[1] ⓘ, Radek Plašil[1] ⓘ, and Juraj Glosík[1] ⓘ

[1] Department of Surface and Plasma Science, Faculty of Mathematics and Physics, Charles University, Prague, V Holešovičkách 2, 180 00, Czech Republic; stepan.roucka@mff.cuni.cz

[2] Department of Physics and CAMOST, Indian Institute of Science Education and Research (IISER) Tirupati, Andhra Pradesh 517507, India

*Received 2023 September 3; revised 2023 November 6; accepted 2023 November 9; published 2023 December 14*

Abstract

The formation of nitrogen hydrides in the interstellar medium is initiated by the nearly thermoneutral reaction of $N^+ + H_2 \rightarrow NH^+ + H$. Here, we experimentally determine the enthalpy of this reaction using the principle of detailed balance from a measurement of the rate coefficient of the reverse reaction $NH^+ + H \rightarrow N^+ + H_2$. The measurements were carried out in a linear radiofrequency 22-pole trap combined with an effusive beam source of atomic hydrogen at temperatures between 10 and 100 K. The resulting ground-state energy difference (or reaction enthalpy at 0 K) of $\Delta E^0 = (18 \pm 4)$ meV confirms that there are no significant energy barriers on the reaction path.

Unified Astronomy Thesaurus concepts: Astrochemistry (75); Reaction rates (2081); Laboratory astrophysics (2004); Experimental data (2371); Molecular data (2259); Small molecules (2267); Molecular physics (2058)

1. Introduction

This work aims to resolve the longstanding question of the enthalpy of the nearly thermoneutral reaction

$$N^+ + H_2 \xrightarrow{k_f} NH^+ + H, \tag{1}$$
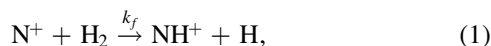
which initiates the formation of nitrogen hydrides in interstellar clouds (Le Gal et al. 2014; Gerin et al. 2016). We will evaluate the reaction enthalpy at 0 K, which is equal to the energy difference between the product and reactant ground states, ΔE^0. This quantity is an essential parameter in calculations of state-specific NH^+ formation rate coefficients in astrochemical models (Grozdanov et al. 2016; Gómez-Carrasco et al. 2022). At temperatures relevant to the chemistry of molecular clouds (Millar 2015), the temperature dependence of the rate coefficient, k_f, of this forward reaction can be represented by the Arrhenius dependence, $k_f = k^0 \exp(-E_A/(k_B T))$, with activation energy $E_A \approx 19$ meV (Marquette et al. 1985; Plašil et al. 2022). The presence of activation energy indicates that the reaction cross section has a certain threshold energy E_T (Menzinger & Wolfgang 1969). However, neither the activation energies nor the threshold energies of cross sections can be directly identified with the reaction enthalpy, as the data can also be explained by the presence of energy barriers. To elucidate the issue, the variation of the activation energy with the internal excitation and isotopic composition of reactants has been studied in a number of experiments (Marquette et al. 1985, 1988; Gerlich 1993; Zymak et al. 2013; Plašil et al. 2022) and some have also deduced the threshold energy (Ervin & Armentrout 1987; Marquette et al. 1988; Gerlich 1993; Tosi et al. 1994). A notable result was obtained by Tosi et al. (1994), who observed that the change of the energy threshold due to

deuteration cannot be explained by the different zero-point energies of the deuterated species, suggesting that the energy threshold is not purely due to reaction enthalpy and an energy barrier is involved. On the other hand, several studies (Adams & Smith 1985; Marquette et al. 1988; Plašil et al. 2022), have observed isotope effects consistent with the hypothesis of no barrier. The recent study by Plašil et al. (2022) shows that the available data are compatible with the hypothesis of no reaction barrier when only low-temperature thermal reaction rate coefficients with known error estimates are taken into account. The isotopic variation of activation energies in accordance with the hypothesis of the absence of energy barriers is a strong indication in favor of this hypothesis.

The reaction enthalpy can, in principle, be calculated as the difference between the H_2 and NH^+ dissociation energies. However, despite the recent theoretical and experimental works (Tarroni et al. 1997; Hübers et al. 2009; Shi et al. 2009; Lecointre et al. 2010; Beloy et al. 2011; Zhang et al. 2017; Yang et al. 2019; Ghosh et al. 2022; Gómez-Carrasco et al. 2022), the dissociation energy of NH^+ has not been determined with sufficient precision yet and the most recent theoretical reaction studies still approximate the energy difference with the experimental activation energies (Gómez-Carrasco et al. 2022). We have therefore chosen an experimental approach to study the reaction endothermicity by measuring the rate coefficient k_r of the reverse reaction

$$NH^+ + H \xrightarrow{k_r} N^+ + H_2. \tag{2}$$
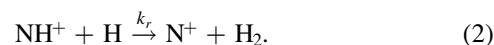
Knowing the forward and reverse thermal rate coefficients and accounting for all the relevant states of the NH_2^+ system (see Figure 1), we can calculate ΔE^0 using the detailed balance principle.

The experiments were carried out in the Atomic Beam with 22-pole Trap instrument (AB-22PT; Gerlich 1992, 2012; Borodi et al. 2009; Plasil et al. 2011; Roučka et al. 2015). The NH^+ ions were produced by electron bombardment from two different precursor gas mixtures in the storage ion source
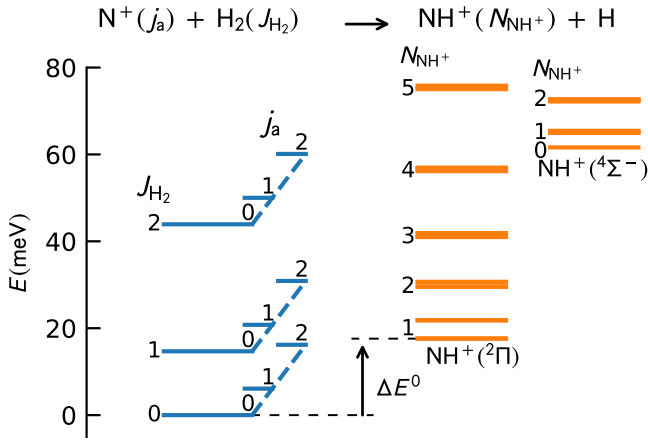
Figure 1. Energy levels of the NH_2^+ system. The energies of the reactants as a function of the N^+ fine-structure state (j_a) and H_2 rotational state (J_{H_2}) are indicated on the left. The energies of the products as a function of the NH^+ rotational state are shown for the two lowest electronic states of NH^+. The rotational states of NH^+ are labeled by the rotational angular momentum quantum number N_{NH^+}. See the text for details of the internal structure calculations. The present value of $\Delta E^0 = 17.6$ meV is indicated in the figure.

Figure 2. Measured numbers of trapped ions, N_i, as a function of trapping time t, showing the loss of the $^{14}NH^+/^{15}N^+$ ions (squares) and formation of the N^+ ions (circles) in the trap. The curves represent least-squares fits of the data with a kinetic model. The data were measured with the H beam *on* (closed symbols and solid lines) and H beam *off* (open symbols and dashed lines). The fitted numbers of $^{14}NH^+$ and $^{15}N^+$ in the measurement with the H beam *on* are indicated by the dotted lines. The measurement was performed at ion and atom temperatures of $T_{NH^+} = 26$ K, $T_H = 75$ K, with an H number density of $n_H = 3.2 \times 10^7 \, cm^{-3}$.

(Gerlich 1992)—either N_2: H_2 or NH_3:He mixtures in pressure ratios of 1: 2 or 1: 10, respectively (with identical resulting rate coefficients within the error margin). After mass selection, the ions were injected into a linear 22-pole radiofrequency trap, where they were cooled by collisions with helium buffer gas. To freeze out the N_2 or NH_3 leaking from the ion source and to avoid parasitic reactions with these species, the trap was kept at temperatures $T_{22PT} < 30$ K. Based on our previous studies of endothermic reactions (Mulin et al. 2015; Roučka et al. 2018; Plašil et al. 2022) and photodetachment spectroscopy (Plašil et al. 2023), we assume that neither the translational nor the internal temperatures of NH^+ exceed the trap temperature by more than 10 K under the present operating conditions. We therefore denote both temperatures as T_{NH^+}, which is given as $T_{NH^+} = T_{22PT} + (5 \pm 5)$ K. The H atoms were produced in a radiofrequency discharge in pure H_2 and they were passing through a cold nozzle (accommodator) with temperature T_{acc} in the range from 7 to 150 K. The H atom temperature T_H is close to T_{acc} (Borodi et al. 2009) and we assume $T_H = T_{acc}$. The atoms exit the accommodator in an effusive beam, which passes through the trap and can be blocked using a mechanical shutter.

The effective translational temperature T_t of the collisions between H atoms with mass M_H and NH^+ ions with mass M_{NH^+} is given as (Light et al. 1969; Gerlich & Horning 1992; Paul et al. 1995) $T_t = (T_H M_{NH^+} + T_{NH^+} M_H)/(M_{NH^+} + M_H)$. The most relevant parameter for determining the rate coefficients of endothermic reactions is the total available collisional energy—the sum of the translational and internal energies $E_{coll}(T_{NH^+}, T_H) = E_{int}(T_{NH^+}) + \frac{3}{2}k_B T_t$. We therefore define the corresponding collisional temperature T_{coll} through the following implicit formula, $E_{int}(T_{coll}) + \frac{3}{2}k_B T_{coll} = E_{coll}$, as the temperature of hypothetical thermal reactants with total collisional energy E_{coll}.

The effective number density of H atoms, n_H, was determined by chemical probing with CO_2^+ using the reaction $CO_2^+ + H \rightarrow HOC^+ + O$ (Borodi et al. 2009). The n_H calibration and reaction measurements were always carried out at similar values of the trap temperature, effective trapping potential, and accommodator temperature in order to maintain
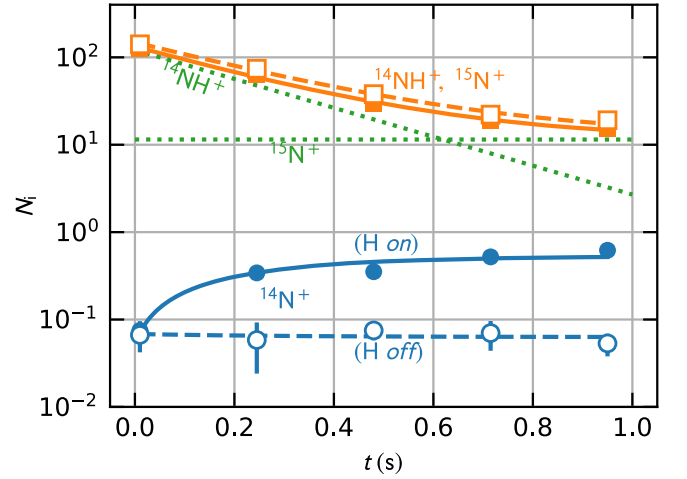
the same overlap of the H beam with the ion cloud and the level of dissociation (Roučka et al. 2015).

2. Results

The typical experimental data are shown in Figure 2. Every measurement is performed with the beam shutter open (H *on*) and closed (H *off*) to resolve the reactions with H atoms from other background reactions. Since our quadrupole mass filter cannot resolve ions with the same number of nucleons, there is also a minor amount of $^{15}N^+$ isotope mixed in with the studied $^{14}NH^+$ ions. The dominant loss process for the $^{14}NH^+$ ions is the fast hydrogen abstraction reaction with the background H_2 gas (Rednyk et al. 2019):

$$NH^+ + H_2 \rightarrow NH_2^+ + H, \tag{3}$$

whereas the $^{15}N^+$ are destroyed by the much slower reaction (1). This is manifested by the bi-exponential decay of the number of ions with $m/z = 15$. These different loss rates allow us to resolve $^{14}NH^+$ from $^{15}N^+$ in the data analysis. The loss of $^{15}N^+$ on the timescale of our experiment is practically negligible and we assume that its reaction rate coefficient with H_2 is equal to that of $^{14}N^+$ (Zymak et al. 2013).

By least-squares fitting (Newville et al. 2014, 2020) of the measured data with a kinetic model that includes reactions (1), (2), and (3), we obtain the rates of N^+ production from NH^+ with the beam *on* and *off* (r_{on} and r_{off}, respectively), where r_{off} is typically close to zero (see Figure 2). The production rates of N^+ due to the interaction of NH^+ with H atoms are calculated as $r = r_{on} - r_{off}$. The rate coefficients of the reverse reaction are finally obtained by dividing the rate with the H atom number density calibrated at equivalent conditions using chemical probing.

The measurements were performed at four H atom temperatures—7, 50, 75, and 100 K—and T_{NH^+} varied from 15 to 30 K. Since the translational temperature T_t is predominantly determined by T_H, we group the results by the accommodator temperature and calculate a weighted average of
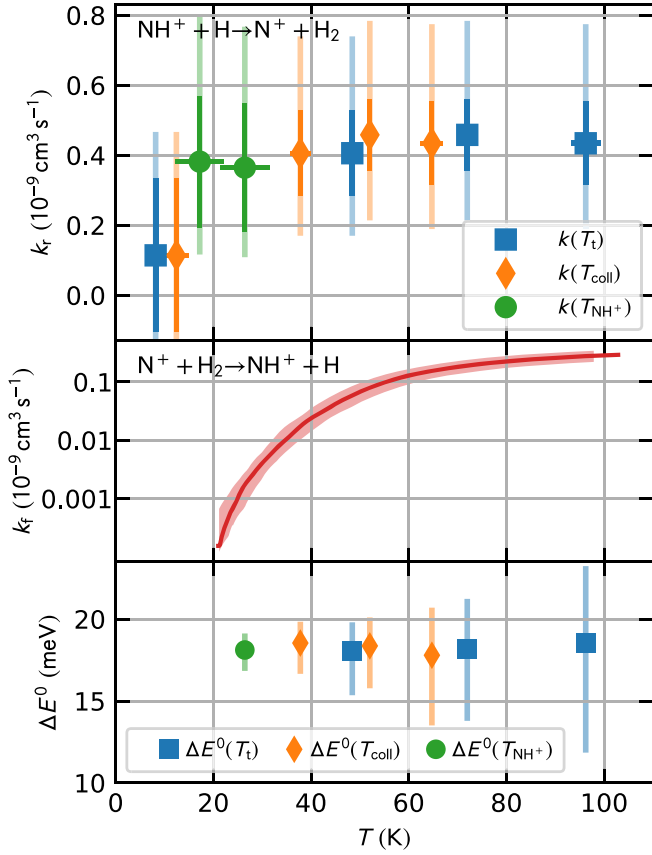
Figure 3. Upper panel: the measured rate coefficients of the reverse reaction as a function of translational, collisional, and NH^+ internal temperatures. The inner error bars indicate the statistical errors, whereas the outer error bars also include the systematic uncertainty due to n_H calibration. Middle panel: the rate coefficient of the forward reaction extracted from the data of Zymak et al. (2013). The systematic error of the data is indicated by the filled band. Lower panel: values of ΔE^0 obtained from the detailed balance principle Equation (5). The overall (systematic + statistical) uncertainties obtained using interval arithmetic from the overall uncertainties of the input data are indicated by the error bars.

the measured reaction rate coefficients in each group. The averaged reverse reaction rate coefficients are plotted as a function of T_t and T_{coll} in the upper panel of Figure 3. We also plot the data as a function of T_{NH^+} (measurements were done mostly at ion temperatures $T_{NH^+} \approx 17$ K and 27 K). The data point at the lowest T_t and T_{coll} ($T_H = 7$ K) has large statistical uncertainty due to the low number density of H atoms in these conditions. The reaction rate coefficients have no significant dependence on temperature. Hence, the reverse reaction has no significant activation energy.

3. Endothermicity Analysis

To obtain quantitative information about the reaction enthalpy, we employ the principle of detailed balance. The full derivation of this principle from quantum mechanics can be found, e.g., in Henriksen & Hansen (2008), Light et al. (1969), and Sakurai & Napolitano (2010). For a general bimolecular reaction $A + B \underset{k_r}{\overset{k_f}{\rightleftharpoons}} C + D$, the forward and reverse reaction rate coefficients are related by the formula

$$\frac{k_f}{k_r} = \left(\frac{\mu_{CD}}{\mu_{AB}}\right)^{3/2} \frac{q_C q_D}{q_A q_B} \exp\left(-\frac{\Delta E^0}{k_B T}\right), \qquad (4)$$

where q_X denotes the internal partition sum of species X and μ_{XY} is the reduced mass of species X and Y (Light et al. 1969).

For H atoms, we take into account the nuclear spin contribution $q_H^{NS} = 2I + 1 = 2$ ($I = 1/2$ for ^{1}H) and the electron spin multiplicity $q_H^S = 2S + 1 = 2$ of the ^{2}S ground state, which leads to $q_H = q_H^{NS} q_H^S = 4$. For N^+ ions, $q_{N^+} = q_{N^+}^{NS} q_{N^+}^{FS}$, where $q_{N^+}^{NS} = 2I + 1 = 3$ ($I = 1$ for ^{14}N; Fuller 1976) and we sum over the $^3P_{j_a}$ fine-structure (FS) states $q_{N^+}^{FS} = \sum_{j_a=0}^2 (2j_a + 1)\exp(-E_{j_a}/k_B T)$, with FS energies E_{j_a} (Kramida et al. 2020). The partition sum of H_2 is calculated over the five lowest rotational states of the vibrational ground state, accounting for the different nuclear spin multiplicities g_J of odd and even (ortho and para) rotational states, $q_{H_2} = \sum_J g_J (2J + 1)\exp(-E_J/k_B T)$, where $g_J = 1$ and 3 for even and odd J, respectively. The H_2 rotational energies E_J are calculated from the molecular constants in Huber & Herzberg (1979). In the case of NH^+, we consider the vibrational ground states of the two lowest electronic states, $^2\Pi$ and $^4\Sigma^-$, where we account for the rotational states with $J \leqslant 19/2$ according to the effective Hamiltonian of Kawaguchi & Amano (1988). We checked that the neglect of the higher energy levels of NH^+ and H_2 does not influence the results of our analysis. The nuclear spin partition function of NH^+ is the product of the hydrogen and nitrogen nuclear spin partition functions, $q_{NH^+}^{NS} = q_H^{NS} q_{N^+}^{NS} = 6$.

When the partition sums are known, we can express ΔE^0 from the measured forward and reverse reaction rate coefficients by applying Equation (4) to reaction (1) as

$$\Delta E^0 = k_B T \ln\left(\frac{k_r}{k_f}\left(\frac{\mu_{NH^+,H}}{\mu_{N^+,H_2}}\right)^{3/2} \frac{q_{NH^+} q_H}{q_{N^+} q_{H_2}}\right). \qquad (5)$$

To evaluate k_f, we first calculate the rate coefficients of reaction (1) with ortho- and para-H_2 from the experimental data with normal and para-enriched H_2 (Zymak et al. 2013), and we take k_f as a weighted average of the state-specific reaction rate coefficients over the thermal population of H_2 nuclear spin states. The systematic uncertainties are not provided by Zymak et al. (2013) and we account for the typical 20% uncertainty of pressure determination and temperature uncertainty defined as $T_{coll} = T_{22PT} + (5 \pm 5)$ K. The thermal rate coefficient of the forward reaction can be obtained down to approximately 20 K (see Figure 3). At lower temperatures, the rate coefficient for reaction with para-H_2 is below the noise level in the measurements with para-enriched H_2. Hence, the reaction enthalpy cannot be extracted from the present data obtained at 7 K accommodator temperature.

When calculating ΔE^0 from Equation (5), we assumed that the temperature in the present experiment is equal to either T_t or T_{coll}. This corresponds to two extreme cases: if we take $T = T_t$, we assume that the internal energy of NH^+ is not relevant for promoting the (possibly endothermic) reverse reaction. Conversely, assuming $T = T_{coll}$ means that the internal energy is equivalent to translational energy in promoting the reverse reaction. For completeness, we also consider the case $T = T_{NH^+}$, i.e., that only the internal energy is relevant.

As expected, the detailed balance analysis leads to positive ΔE^0, i.e., the reverse reaction is exothermic. The obtained data shown in the lower panel of Figure 3 as a function of T_t, T_{coll}, or T_{NH^+} do not depend on temperature, in accordance with the
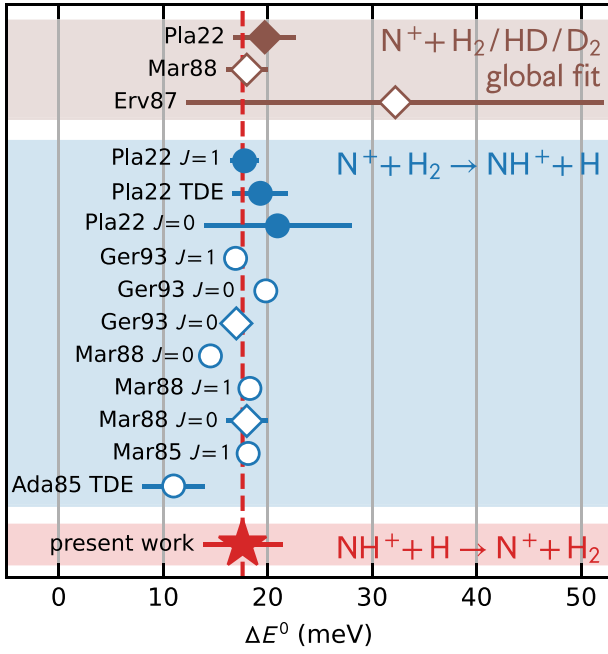
Figure 4. Comparison of the reaction enthalpy determined in the present study with the upper estimates obtained in previous studies of the forward reaction: Pla22 (Plašil et al. 2022), Ger93 (Gerlich 1993), Mar88 (Marquette et al. 1988), Erv87 (Ervin & Armentrout 1987), Mar85 (Marquette et al. 1985), and Ada85 (Adams & Smith 1985). The circles indicate activation energies and the diamonds indicate evaluated reaction enthalpies with the assumption of no barrier. The values labeled as "global fit" were evaluated by combining the experimental data for multiple isotopic variants of the forward reaction.

fact that ΔE^0 is a constant. Averaging the data obtained at different accommodator temperatures leads to $\Delta E^0(T_t) = 18.3^{+3.1}_{-4.5}$ meV, $\Delta E^0(T_{coll}) = 18.4^{+1.8}_{-2.8}$ meV, and $\Delta E^0(T_{NH^+}) = 18.1^{+1.0}_{-1.3}$ meV when assuming $T = T_t$, $T = T_{coll}$, and $T = T_{NH^+}$, respectively. The averages are obtained as arithmetic means of the data and the stated error estimates represent the mean upper/lower systematic error bounds due to the systematic uncertainties (40% of n_H and $T_{NH^+} \pm 5$ K). Regardless of our assumptions on temperature, ΔE^0 is contained between 13.8 and 21.4 meV, i.e., our experimental value of ΔE^0 can be represented as $\Delta E^0 = (17.6 \pm 3.8)$ meV or, after rounding, as

$$\Delta E^0 = (18 \pm 4) \text{ meV}. \qquad (6)$$

The vibrationless energy change ΔE_e (Grozdanov et al. 2016; Plašil et al. 2022) can be calculated by correcting for the zero-point vibrational energies (ZPEs) of reactants and products. Subtracting the ZPE of NH^+ (186.9 meV Colin 1989) and adding the ZPE of H_2 (270.2 meV Huber & Herzberg 1979) leads to

$$\Delta E_e = (101 \pm 4) \text{ meV}. \qquad (7)$$

The resulting vibrationless energy change is consistent with $\Delta E_e = (103 \pm 3)$ meV obtained by Plašil et al. (2022) in the ion trap study of $N^+ + HD/D_2$ reactions under the assumption of no reaction barriers.

The measured value of the reaction enthalpy ΔE^0 can be utilized to calculate the dissociation energy of NH^+ in the $^2\Pi$ ground state toward the $N^+ + H$ asymptote as

$$D_0(N^+\text{--}H, \,^2\Pi)$$
$$= D_0(H\text{--}H, \,^1\Sigma_g) - \Delta E^0 = (4460 \pm 4) \text{ meV}, \qquad (8)$$

where the H_2 dissociation energy is $D_0(H - H, \,^1\Sigma_g) = 4478.1$ meV (Liu et al. 2009). This value is in agreement with the theoretically calculated dissociation energy $D_0(N^+\text{--}H, \,^2\Pi) = 4462$ meV (Tarroni et al. 1997). The dissociation energy toward the $N + H^+$ asymptote can be calculated from the known ionization potentials (IPs) of H and N (Kramida et al. 2020), resulting in $D_0(N\text{--}H^+, \,^2\Pi) = D_0(N^+\text{--}H, \,^2\Pi) + IP(H) - IP(N) = (3525 \pm 4)$ meV, in agreement with the experimental values (3531 ± 3) meV of Adams & Smith (1985) and (3524 ± 3) meV of Marquette et al. (1988), which were obtained from measurements of k_f with para-enriched and normal H_2, HD, and D_2 with the assumption of no energy barrier. Since the process $NH^+ (^2\Pi) \rightarrow N (^4S) + H^+(^1S)$ involves an electronic transition, some works report instead the adiabatic energy of dissociation from the $NH^+ (^4\Sigma^-)$ state (Tarroni et al. 1997; Amero & Vázquez 2005). This can be calculated as $D_0(N\text{--}H^+, \,^4\Sigma^-) = D_0(N\text{--}H^+, \,^2\Pi) - \Delta E_{\Sigma\Pi} = (3481 \pm 4)$ meV, where $\Delta E_{\Sigma\Pi} = 44.0$ meV is the energy difference between the lowest levels of the $^4\Sigma^-$ and $^2\Pi$ electronic states (Kawaguchi & Amano 1988). The theoretically determined value $D_0(N\text{--}H^+, \,^4\Sigma^-) = 3496$ meV (Tarroni et al. 1997) is in satisfactory agreement with our data, considering that the theory neglects the spin–orbit interaction. More information concerning NH^+ dissociation energies can be found in Amero & Vázquez (2005) and Tarroni et al. (1997).

4. Discussion and Conclusion

We have used the principle of detailed balance to derive the enthalpy of reaction (1) from the measurements of forward and reverse reaction rate coefficients. This method is accurate if the reactants both in the forward and reverse reaction measurements are in thermal equilibrium. In our study, we had to deal with a few deviations from thermal equilibrium:

(1) The nuclear spin states of H_2 in the k_f measurement were not in equilibrium. However, measurements with two different nuclear spin state populations (Zymak et al. 2013) allowed us to derive the thermal reaction rate coefficients.

(2) The FS-level population of N^+ in the k_f measurement was not known. However, our experimental results (Zymak et al. 2013; Plašil et al. 2022) are compatible with the assumption that the FS of N^+ ions is relaxed efficiently in collisions with He, and this conclusion is also supported by a recent theoretical prediction of relatively fast FS relaxation in collisions of N^+ with H_2 and He (Gueguen & Lique 2023).

(3) The internal and translational temperatures, T_{NH^+} and T_t, are not in equilibrium, but we show in Figure 3 that the obtained reaction enthalpy is independent of the assumptions concerning the role of the translational and internal temperature of the reactants, owing to the fact that the reverse reaction rate coefficients are nearly constant throughout the studied temperature range.

The present value of ΔE^0 is compared to the previously measured activation energies, E_A, and energy thresholds, E_T, of the forward reaction in Figure 4. If there are no barriers on the reaction paths, E_T should be equal to ΔE^0 and E_A should converge to ΔE^0 at low temperatures ($k_B T \ll E_A$; Menzinger & Wolfgang 1969). The good agreement of the previously determined E_A and E_T with the measured value of ΔE^0 confirms that the assumption of no barriers is valid (the agreement with the data of Marquette et al. 1985; Gerlich 1993

with unknown uncertainties cannot be statistically evaluated). The height of the hypothetical energy barrier can be calculated as $E_b = E_A - \Delta E^0$ and using the most recent value of $E_A = (19.3 \pm 2.7)$ meV for H_2 in thermodynamic equilibrium (TDE; Plašil et al. 2022) leads to $E_b = (2 \pm 5)$ meV. Therefore, the height of the possible barrier is, within the accuracy of our measurement, equal to zero. This result confirms that the interpretation of the activation energy as reaction endothermicity in the previous theoretical (Grozdanov & McCarroll 2015; Grozdanov et al. 2016; Yang et al. 2019; Gómez-Carrasco et al. 2022) and astrochemical (Dislaire et al. 2012; Roueff et al. 2015) studies was justified, providing solid ground for further research of the $N^+ + H_2$ collision system.

Acknowledgments

ORCID iDs

Štěpán Roučka https://orcid.org/0000-0002-2419-946X
Serhiy Rednyk https://orcid.org/0000-0002-0408-0170
Thuy Dung Tran https://orcid.org/0000-0002-9894-1647
Artem Kovalenko https://orcid.org/0000-0001-9521-6821
Sunil S. Kumar https://orcid.org/0000-0002-1646-0517
Petr Dohnal https://orcid.org/0000-0003-0341-0382
Radek Plašil https://orcid.org/0000-0001-8520-8983
Juraj Glosík https://orcid.org/0000-0002-2638-9435

References

Adams, N. G., & Smith, D. 1985, CPL, 117, 67
Amero, J. M., & Vázquez, G. J. 2005, IJQC, 101, 396
Beloy, K., Kozlov, M. G., Borschevsky, A., et al. 2011, PhRvA, 83, 062514
Borodi, G., Luca, A., & Gerlich, D. 2009, IJMSp, 280, 218
Colin, R. 1989, JMoSp, 136, 387
Dislaire, V., Hily-Blant, P., Faure, A., et al. 2012, A&A, 537, A20
Ervin, K. M., & Armentrout, P. B. 1987, JChPh, 86, 2659
Fuller, G. H. 1976, JPCRD, 5, 835
Gerin, M., Neufeld, D. A., & Goicoechea, J. R. 2016, ARA&A, 54, 181
Gerlich, D. 1992, in Advances in Chemical Physics: State-Selected and State-To-State Ion-Molecule Reaction Dynamics, Part 1. Experiment, Volume 82, ed. C.-Y. Ng et al. (Hoboken, NJ: Wiley), 1
Gerlich, D. 1993, J. Chem. Soc., Faraday Trans., 89, 2199
Gerlich, D., & Horning, S. 1992, ChRv, 92, 1509
Gerlich, D., Jusko, P., Roučka, Š., et al. 2012, ApJ, 749, 22
Ghosh, R., Chakrabarti, K., & Choudhury, B. S. 2022, PSST, 31, 065005
Gómez-Carrasco, S., Félix-González, D., Aguado, A., & Roncero, O. 2022, JChPh, 157, 084301
Grozdanov, T. P., & McCarroll, R. 2015, JPCA, 119, 5988
Grozdanov, T. P., McCarroll, R., & Roueff, E. 2016, A&A, 589, A105
Gueguen, M., & Lique, F. 2023, MNRAS, 522, 6251
Henriksen, N. E., & Hansen, F. Y. 2008, Theories of Molecular Reaction Dynamics: The Microscopic Foundation of Chemical Kinetics (Oxford: Oxford Univ. Press)
Huber, K. P., & Herzberg, G. 1979, Molecular Spectra And Molecular Structure, Vol. IV, Molecular Spectra And Molecular Structure: Constants Of Diatomic Molecules (New York: Van Nostrand-Reinhold)
Hübers, H.-W., Evenson, K. M., Hill, C., & Brown, J. M. 2009, JChPh, 131, 034311
Kawaguchi, K., & Amano, T. 1988, JChPh, 88, 4584
Kramida, A., Ralchenko, Y., & Reader, J. 2020, NIST Atomic Spectra Database, v5.8, National Institute of Standards and Technology, doi:10.18434/T4W30F
Lecointre, J., Jureta, J. J., & Defrance, P. 2010, JPhB, 43, 105202
Le Gal, R., Hily-Blant, P., Faure, A., et al. 2014, A&A, 562, A83
Light, J. C., Ross, J., & Shuler, K. E. 1969, in Kinetic Processes in Gases and Plasmas, ed. A. R. Hochstim (New York: Academic), 281
Liu, J., Salumbides, E. J., Hollenstein, U., et al. 2009, JChPh, 130, 174306
Marquette, J. B., Rebrion, C., & Rowe, B. R. 1988, JChPh, 89, 2041
Marquette, J. B., Rowe, B. R., Dupeyrat, G., & Roueff, E. 1985, A&A, 147, 115
Menzinger, M., & Wolfgang, R. 1969, AngCh, 8, 438
Millar, T. J. 2015, PSST, 24, 043001
Mulin, D., Roučka, Š., Jusko, P., et al. 2015, PCCP, 17, 8732
Newville, M., Otten, R., Nelson, A., et al. 2020, Lmfit/Lmfit-Py, v1.0.1, Zenodo, doi:10.5281/zenodo.3814709
Newville, M., Stensitzki, T., Allen, D. B., & Ingargiola, A. 2014, LMFIT: Non-linear Least-square Minimization and Curve-fitting for Python, v0.8.0, Zenodo, doi:10.5281/zenodo.11813
Paul, W., Lücke, B., Schlemmer, S., & Gerlich, D. 1995, IJMSI, 149, 373
Plasil, R., Mehner, T., Dohnal, P., et al. 2011, ApJ, 737, 60
Plašil, R., Roučka, Š., Kovalenko, A., et al. 2022, ApJ, 941, 144
Plašil, R., Uvarova, L., Rednyk, S., et al. 2023, ApJ, 948, 131
Rednyk, S., Roučka, Š., Kovalenko, A., et al. 2019, A&A, 625, A74
Roueff, E., Loison, J. C., & Hickson, K. M. 2015, A&A, 576, A99
Roučka, Š., Mulin, D., Jusko, P., et al. 2015, J. Phys. Chem. Lett., 6, 4762
Roučka, Š., Rednyk, S., Kovalenko, A., et al. 2018, A&A, 615, L6
Sakurai, J. J., & Napolitano, J. J. 2010, Modern Quantum Mechanics (2nd ed.; Reading, MA: Addison-Wesley)
Shi, D., Zhang, J., Yu, B., et al. 2009, JMoSt, 896, 116
Tarroni, R., Palmieri, P., Mitrushenkov, A., Tosi, P., & Bassi, D. 1997, JChPh, 106, 10265
Tosi, P., Dmitriev, O., Bassi, D., Wick, O., & Gerlich, D. 1994, JChPh, 100, 4300
Yang, Z., Wang, S., Yuan, J., & Chen, M. 2019, PCCP, 21, 22203
Zhang, Q.-Q., Yang, C.-L., Wang, M.-S., Ma, X.-G., & Liu, W.-W. 2017, AcSpA, 185, 365
Zymak, I., Hejduk, M., Mulin, D., et al. 2013, ApJ, 768, 86